Int J Fract (2009) 157:13–32
DOI 10.1007/s10704-008-9297-0

ORIGINAL PAPER

Integral equations and nonlocal damage theory: a numerical implementation using the BDEM

V. Mallardo

Received: 18 March 2008 / Accepted: 24 November 2008 / Published online: 25 December 2008

Abstract In this paper the integral equation approach is developed to describe elastic-damaging materials. An isotropic damage model is implemented to study nonlinear structural problems involving localisation phenomena. Especially for the cases that exhibit stress or strain concentrations, an integral approach can be recommended. Besides, the technique is able to represent well high gradients of stress/strain. The governing integral equations are discretised by using quadratic isoparametric elements on the boundary and quadratic continuous/discontinuous cells in the zone where the nonlinear phenomenon occurs. Two numerical examples are presented to show the physical correctness and efficiency of the proposed procedure. The results are compared with the local theory and they turn out to be free of the spurious sensitivity to cell mesh refinement.

Keywords Damage · Nonlocal · Integral equations · Arclength

1. Introduction

Quasibrittle materials, such as concrete, rock, tough ceramics or ice, are characterised by the development of nonlinear fracture process zones, which can be macroscopically described as regions of highly localised strains. The classical linear elastic fracture mechanics cannot be directly applied to such materials, because of the existence of a narrow fracture process zone containing a large number of distributed microcracks at the fracture front. In the last twenty years Continuum Damage Mechanics has grown as a link between the classical Continuum and the Fracture Mechanics. This approach tries to model the development, the growth and finally the coalescence of microdefects which could lead to the occurring of macrocracks and eventually of rupture. One of the most commonly used damage models introduces an arbitrary variable tensor to model the growth and the diffusion of the microcracks inside the solid. Such a tensor is introduced in the constitutive equations in order to describe the region of the body in which a degradation of the material elastic properties due to the microcracking phenomenon occurs. In practical application the damage is often considered isotropic, i.e. a scalar variable d rather than a tensor is used. The development of material damage produces a strain softening behaviour: after a threshold of stress or strain is reached, the model exhibits a decreasing stress with increasing strain. The problem is that modelling the softening materials as elastic-damaging fails because, as pointed out already by Hadamard, the dynamic initial-boundary-value problem changes its type from hyperbolic to elliptic and becomes ill posed. The finite element (FE) numerical solution is unobjective with respect to the choice of the mesh and, upon the mesh refinement, it converges to a solution with a vanishing energy dissipation. To

V. Mallardo (✉)
Department of Architecture, University of Ferrara,
via Quartieri 8, 44100 Ferrara, Italy
e-mail: mlv@unife.it

overcome such drawbacks some regularisation techniques have been proposed. One of these is based on the formulation of a nonlocal continuum. The idea comes from the assumption that standard Continuum Mechanics theories are not appropriate when the microscopic material heterogeneity is characterised by an internal length which cannot be neglected in comparison with the macroscopic length of the structure. The material cannot be treated as a continuum any more, but the model needs to be enriched in order to keep in count that the range of the microscopic interaction forces has to be considered long with respect to the macroscopic level. The idea of the integral-type nonlocal material model is that the constitutive law at a point of a continuum involves weighted averages of a state variable over a certain neighbourhood of that point. A characteristic length is also introduced to control the spread of the nonlocal weight function. A lot of work has been done in the FE context; see for example Jirásek (1998) for a critical comparison of approaches of nonlocal models for damage and fracture, Jirásek and Rolshoven (2003) for the description of various integral-type nonlocal plasticity models and Bažant and Jirásek (2002) for an interesting survey of progress of nonlocal integral formulations of plasticity and damage. In the formulation of a nonlocal model, several choices have to be made regarding the definition of the variable to be treated as nonlocal, the definition of the weight function and the definition of the characteristic length. In Comi and Perego (2001) the issue of the relation between the symmetry of the tangent operator in a finite element approximation and the choice in the constitutive variable to average is performed. In Jirásek and Patzak (2002) the Authors present and discuss a general framework for a consistent derivation of the nonlocal tangent stiffness: such a matrix turns out to be nonsymmetric but the lack of symmetry, in the Authors' opinion, cannot be considered as a substantial drawback. In Borino et al. (2003) a thermodynamically consistent formulation for nonlocal damage models is presented: the main feature of the proposed scheme is that the nonlocal integral operator is self-adjoint at every point of the solid, including zones near to the boundary of the solid. The very first coupling of the Boundary Element Method (BEM) with nonlocal operators is given by Garcia et al. (1999). The damage model by Mazars is involved and the nonlocal operator is applied to the equivalent strain of the damage function. The main limitation of the paper is the application of the grid damage model: the damage is assumed constant in every internal cell, therefore the Boundary Integral equations are written by collocating in every node of the boundary cell and compatibility and equilibrium equations are imposed across the boundary between two adjacent cells. There is an enormous increase of computational effort due to the arising system of equations which makes the procedure disadvantageous when compared to a classical FE approach. It must be pointed out that integral formulations are very suited to represent high gradients and they can be recommended in the cases which exhibit stress or strain concentrations. Both the BEM and the Boundary/Domain Element Method (BDEM), in fact, are able to furnish a very precise evaluation of the stress tensor in any internal point and to reduce tremendously the number of the unknowns when the nonlinear zone is relatively small in comparison with the overall size of the finite domain. In order to deal with damage it is necessary to implement an arclength control technique. The problem is addressed in Mallardo and Alessandri (2004) where the arclength procedure is combined with the BDEM in physically nonlinear problems. The arclength constraint, added to the governing integral equations, forms a nonlinear system of equations which is solved by applying directly the Newton-Raphson method. Only in 2002–2003 have Lin et al. (2002) and Sládek et al. (2003) incorporated an integral type nonlocal strain softening localisation limiter into the BDEM; nevertheless, they use a formulation which both gives some locking effects in FE and they cannot deal with snap-back behaviours. In Alessandri et al. (2000) a nonlocal integral formulation for elastic-damaging materials is presented. In the paper only the nonlocal formulation and the coupling with BDEM are presented. Some numerical results are given in Mallardo (2004) but the nonlocal approach is not completely and adequately developed. Benallal et al. (2006) proposed a two-dimensional (2D) nonlocal damage model in the Boundary Element (BE) context. Linear boundary elements and linear domain cells are implemented. In Sfantos and Aliabadi (2007a) an interesting cohesive grain boundary integral formulation is proposed for simulating intergranular microfracture evolution in polycrystalline brittle materials. In Sfantos and Aliabadi (2007b) a multi-scale boundary element method for modeling damage is proposed.

The present study deals with a thermodynamically consistent formulation for integral type nonlocal damage models coupled with the BDEM. The boundary is

discretised into quadratic continuous elements whereas the part of domain in which the nonlinear term is expected to occur is discretised into quadratic quadrilateral/triangular cells. Proper procedures are developed in order to handle the involving singular integrals. The strain energy release rate is taken as the variable to consider as nonlocal. The advantage of such a choice is in the possibility of carrying out all constitutive calculations locally at each cell point despite of the nonlocality of the model. Another consequence is the lack of symmetry of the resulting stiffness tangent matrix, but this is not an actual drawback in the BEs context; in fact, even the classical (collocation) BEM approach leads to a coefficient matrix which is not symmetric at all. In order to keep in count the possibility of any type of structural response an arclength procedure, as implemented by Mallardo (2004), is used.

2. The damage model

Following an idea by Krajcinovic (1996), the nonlinear behaviour of quasi-brittle materials can be phenomenologically represented by continuum damage models in which a tensor **d** gives, for any plane containing the point, the measure of the micro-crack diffusion. The value of such a tensor in any point is related to the ratio between the effective area of the intersection of all microcracks lying in the plane and the area of the intersection of the plane with the representative volume element (RVE). In the present contribution the damage is assumed to be isotropic, i.e. d is scalar, and the formulation is confined to the case of small induced strains. The stress–strain relation can be written in the following way:

$$\boldsymbol{\sigma} = f(d) C^{el} : \boldsymbol{\varepsilon} \tag{1}$$

where C^{el} is the fourth order elastic moduli tensor, $\boldsymbol{\sigma}$ and $\boldsymbol{\varepsilon}$ are the stress and the strain tensor respectively and $f(d)$ is a suitable function of the damage parameter d. Some possibilities are given for $f(d)$. The most common is the linear one:

$$f(d) = 1 - d \tag{2}$$

which satisfies the phenomenological meaning of d. Another choice is the quadratic one:

$$f(d) = (1 - d)^2 \tag{3}$$

Such a position relates d to the reduction of the strain energy release rate, rather than to the reduction of area, due to the diffusion of microcracking.

In order to set the model consistently with thermodynamic principles, it is necessary to introduce the energy per unit of volume Y:

$$Y := \frac{1}{2} \frac{\partial f(d)}{\partial d} \boldsymbol{\varepsilon} : C^{el} : \boldsymbol{\varepsilon} \tag{4}$$

the kinematic internal variable γ and the force X whose definition depends on the way the nonlinear aspect of the phenomenon is described.

By comparison with plasticity, X could be defined as:

$$X = X_1 := h\gamma \tag{5}$$

Another definition is (see Comi and Perego 2001):

$$X = X_2 := k \ln^n \frac{c}{1 - \gamma} \tag{6}$$

where k, c and n are material parameters.

It can be proved (see Comi and Perego 2001; Benvenuti et al. 2002 for details) that both formulations are consistent with thermodynamic principles assuming the existence of an Helmholtz free energy of the form:

$$\psi(\boldsymbol{\varepsilon}, d, \gamma) = \frac{1}{2} \boldsymbol{\varepsilon} : f(d) C^{el} : \boldsymbol{\varepsilon} + \psi^{nl}(\gamma) \tag{7}$$

where the first term is the damage elastic strain energy and the second term (nl stands for non linear) is the energy stored in the microstructure due to the change of the material internal properties. In this context Y and X assume the meaning of thermodynamic force conjugated respectively to d and γ . The expressions (1), (4), (5) and (6) can be obtained by well established procedures based on the assumption that the intrinsic dissipation is equal or greater than zero for any admissible deformation mechanism, be it elastic or damaging, if a suitable expression of the nonlinear part of the free energy is given.

The expressions of ψ^{nl} related to relations (5) and (6) are respectively

$$\psi^{nl}(\gamma) = \psi_1^{nl}(\gamma) = \frac{1}{2} h \gamma^2 \tag{8}$$

$$\psi^{nl}(\gamma) = \psi_2^{nl}(\gamma) = -k(1 - \gamma) \sum_{i=0}^{n} \frac{n!}{i!} \ln^i \left(\frac{c}{1 - \gamma} \right) \tag{9}$$

where by definition $0! = 1$.

The existence of a damage activation function $g(Y, X)$ is now assumed. Under the hypothesis of generalised associative damage behaviour, the damage activation function can be written either as:

$$g(Y, X) = g_1(Y, X) = Y - Y_0 - X \tag{10}$$

or as:

$$g(Y, X) = g_2(Y, X) = Y - X \tag{11}$$

depending on the expression of ψ^{nl} assumed (respectively 8 or 9). The evolution equations read:

$$g(Y, X) \leq 0 \quad \dot{d} = \dot{\lambda}_d = \dot{\gamma}$$
$$\text{with } \dot{\lambda}_d \geq 0 \text{ and } \dot{\lambda}_d \, g = 0 \tag{12}$$

in any point of the body V.

At the generic iteration and at the points where the damage activation function is zero (points $\mathbf{x} \in V_d \subseteq V$), the response is either elastic or damaging and the following relations must hold:

$$\dot{g} \leq 0 \qquad \dot{\lambda}_d \geq 0 \qquad \dot{\lambda}_d \, \dot{g} = 0 \tag{13}$$

Expanding the damage activation function in its rate form leads to:

$$\dot{g}(Y, X) = \frac{\partial g}{\partial Y}\dot{Y} + \frac{\partial g}{\partial X}\dot{X} = \dot{Y} - \dot{X} \tag{14}$$

where:

$$\dot{Y} = \frac{1}{2}\frac{\partial^2 f(d)}{\partial d^2}\boldsymbol{\varepsilon} : C^{el} : \boldsymbol{\varepsilon}\dot{d} + \frac{\partial f(d)}{\partial d}\boldsymbol{\varepsilon} : C^{el} : \dot{\boldsymbol{\varepsilon}} \tag{15}$$

and

$$\dot{X}_1 = \frac{\partial X_1}{\partial \gamma}\dot{\gamma} = h\dot{\gamma} \tag{16}$$

$$\dot{X}_2 = \frac{\partial X_2}{\partial \gamma}\dot{\gamma} = -\frac{kn}{1-\gamma}\dot{\gamma}\ln^{n-1}\left(\frac{c}{1-\gamma}\right) \tag{17}$$

The main difference between the two definitions of the internal variable X conjugate of γ stands in the way the softening branch is described. In fact, it is possible to obtain an analytical solution in the simple case of uniaxial compression/tension test. Figure 1 shows such a difference: it is possible to notice that the Eq. 6 gives a softening branch (Fig. 1b) which asymptotically tends to zero stress.

The nonlocal version of the simple model described above is obtained by substitution of the strain energy rate Y with its nonlocal value. The advantage of this choice for the linear damage model is the possibility of carrying out all constitutive calculation locally in a way which is formally equivalent to the local version, despite of the nonlocality introduced. Other choices are also possible with different physical and computational implications (see for instance Jirásek 1998).

If $Y(\mathbf{x})$ is the local value at a point $\mathbf{x} \in V$, the corresponding nonlocal value is defined by:

$$\overline{Y}(\mathbf{x}) = \int_V W(\mathbf{x}, \mathbf{y}) Y(\mathbf{y}) dV(\mathbf{y}) \tag{18}$$

The weight function $W(\mathbf{x}, \mathbf{y})$ is given by:

$$W(\mathbf{x}, \mathbf{y}) = \frac{W_0(\mathbf{x}, \mathbf{y})}{\overline{W}(\mathbf{x})} \tag{19}$$

where $W_0(\mathbf{x}, \mathbf{y})$ is a monotonically decreasing non-negative function of the distance $r = \|\mathbf{y} - \mathbf{x}\|$ here chosen as the Gauss distribution function, i.e.:

$$W_0(\mathbf{x}, \mathbf{y}) = e^{\frac{-\|\mathbf{x}-\mathbf{y}\|^2}{2l_c^2}} \tag{20}$$

$\overline{W}(\mathbf{x})$ is introduced in order to ensure that uniform damage fields are not modified by the spatial average. This is guaranteed by posing:

$$\overline{W}(\mathbf{x}) = \int_V W_0(\mathbf{x}, \mathbf{y}) dV(\mathbf{y}) \tag{21}$$

i.e. by requiring that:

$$\int_V W(\mathbf{x}, \mathbf{y}) dV(\mathbf{y}) = 1 \qquad \forall \mathbf{x} \in V \tag{22}$$

The parameter l_c in Eq. 20 plays the role of an internal length controlling the nonlocal spatial spread of the damage. The particular nonlocal model here considered has a nonsymmetric stiffness tangent matrix, but two points must be underlined: firstly, a symmetric nonlocal damage formulation is theoretically appealing but

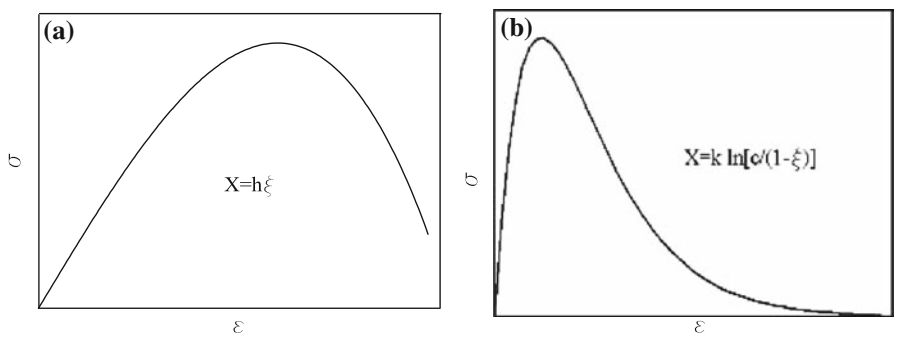

Fig. 1 stress–strain behaviour for the 1-D model. $X = h\xi$ (**a**), $X = k \ln^n \frac{c}{1-\xi}$ (**b**)

less suitable for practical computational purposes than a nonsymmetric one, secondly, the lack of symmetry is present in the classical BEM approach even for the linear elastic case, therefore no more complications are introduced. Another reason of the lack of symmetry of the proposed model comes from the weight function, i.e. $W(\mathbf{x}, \mathbf{y}) \neq W(\mathbf{y}, \mathbf{x})$. Borino et al. (2003) proposed a new averaging weight function which results to be symmetric everywhere.

The numerical results which will be presented are obtained by using the Gauss distribution function given by Eq. 20 and by involving the weight function proposed by Borino et al. (2003). The final values result to be coincident in terms of structural response and damage contour plot.

On the assumptions made, the nonlocal damage activation function becomes:

$$g_1(\overline{Y}, X) = \overline{Y} - Y_0 - X$$
$$g_2(\overline{Y}, X) = \overline{Y} - X \tag{23}$$

whereas the expressions for the flow laws and the damage evolutive laws are not different from the local ones.

3. The boundary integral equations

It is possible to show that the boundary integral equations governing the elastic-damaging problem are similar to the ones involved in the classical elastoplasticity. The relations are presented in rate form in order to keep a unified notation, the time parameter being given by the load increment. Under the assumption of small strains, the total strain can be decomposed into elastic and damaged parts:

$$\dot{\varepsilon}_{ij}(\mathbf{x}) = \dot{\varepsilon}^{el}_{ij}(\mathbf{x}) + \dot{\varepsilon}^{d}_{ij}(\mathbf{x}) = \frac{1}{2}\left[\dot{u}_{i,j}(\mathbf{x}) + \dot{u}_{j,i}(\mathbf{x})\right] \tag{24}$$

The Latin subscripts refer to Cartesian coordinates and the Einstein's notation is adopted, i.e. comma denotes the derivative and repetition implies summation.

The stress tensor rate $\dot{\sigma_{ij}}$ which is related to the elastic strain tensor by:

$$\dot{\sigma}_{ij}(\mathbf{X}) = C^{el}_{ijlm}\dot{\varepsilon}^{el}_{lm} = 2\mu\left(\dot{\varepsilon}^{el}_{ij} + \frac{\nu}{1-2\nu}\delta_{ij}\dot{\varepsilon}^{el}_{kk}\right) \tag{25}$$

where δ_{ij} is the delta Kronecker, ν is the Poisson's ratio and k goes from 1 to 3 in the general 3-D analyses, can be written as:

$$\dot{\sigma}_{ij} := \dot{\sigma}^{el}_{ij} - \dot{\sigma}^{d}_{ij} = C^{el}_{ijlm}\dot{\varepsilon}_{lm} - C^{el}_{ijlm}\dot{\varepsilon}^{d}_{lm} \tag{26}$$

where $\dot{\sigma}^{el}_{ij}$ (named elastic stress tensor rate) and $\dot{\sigma}^{d}_{ij}$ (named damaged stress tensor rate) are the stress tensor rates generated via elastic moduli tensor respectively by the total strain and by the damaging strain.

In the proposed damage model it is easy to show that the stress tensor rate is related to the elastic one by:

$$\dot{\sigma}_{ij} = (1-d)^n\dot{\sigma}^{el}_{ij} - n(1-d)^{n-1}\dot{d}\sigma^{el}_{ij} \tag{27}$$

where $n = 1, 2$ in the case of linear and quadratic damage respectively.

The relation (26) can be written for the traction rate too:

$$\dot{t}_i = \dot{\sigma}_{ij}n_j = \dot{t}^{el}_i - \dot{t}^{d}_i \tag{28}$$

Keeping in count the above propositions, the governing equilibrium equation for the problem under examination (volume forces are neglected):

$$\dot{\sigma}_{ij,j} = 0 \Leftrightarrow \dot{\sigma}^{el}_{ij,j} = \dot{\sigma}^{d}_{ij,j} \tag{29}$$

can be written in terms of displacement rates:

$$(\lambda + \mu)\,\dot{u}_{j,ji}(\mathbf{x}) + \mu\dot{u}_{i,jj}(\mathbf{x}) = \dot{\sigma}^{d}_{ij,j}(\mathbf{x}) \tag{30}$$

where λ and μ are the Lamé elastic constants. It must be said that the representation of the equilibrium equations (29) in terms of stresses rather than displacements (30) results to be more cumbersome to deal with if an integral representation is to be obtained. In fact, the integral representation of the displacement rate satisfying the governing equilibrium equations can be obtained by weighting (29) with the elastostatic fundamental solution due to Kelvin, i.e. with displacement $u^*_{ij}(\mathbf{X}, \mathbf{x})$ and traction $t^*_{ij}(\mathbf{X}, \mathbf{x})$ in the j direction at any point $\mathbf{x}$ of an infinite elastic medium due to a unit point load applied at $\mathbf{X}$ in the i direction. The expression of such an integral representation is:

$$\begin{aligned}\dot{u}_i(\mathbf{X}) = &\int_\Gamma u^*_{ij}(\mathbf{X}, \mathbf{x})\dot{t}_j(\mathbf{x})d\Gamma(\mathbf{x}) \\ &- \int_\Gamma t^*_{ij}(\mathbf{X}, \mathbf{x})\dot{u}_j(\mathbf{x})d\Gamma(\mathbf{x}) \\ &+ \int_\Omega \varepsilon^*_{ijk}(\mathbf{X}, \mathbf{x})\dot{\sigma}^{d}_{jk}(\mathbf{x})d\Omega(\mathbf{x})\end{aligned} \tag{31}$$

where the term ε^*_{ijk} represents the strain tensor corresponding to u^*_{ij}. The fundamental solutions are given in Appendix A.

The relation (31) is a continuous representation of displacements at any point $\mathbf{X} \in \overset{\circ}{\boldsymbol{\Omega}}$ where $\boldsymbol{\Omega}$ is the body

under analysis and Γ is its boundary. Such an expression gives the displacement component rate at any internal point $\mathbf{X}$ once the displacement and the traction fields have been determined on the boundary Γ. The stress state at any point can be obtained in the same way as in plasticity (see for instance Aliabadi 2002, pp. 241–242) by applying the generalised Hooke's law to the elastic part of the total strain rate tensor:

$$\dot{\sigma}_{ij} = \mu(\dot{u}_{i,j} + \dot{u}_{j,i}) + \frac{2\mu\nu}{1-2\nu}\dot{u}_{k,k}\delta_{ij} - \dot{\sigma}^d_{ij} \tag{32}$$

It must be pointed out that the space derivatives, which are necessary to obtain the strain tensor rate from the displacement one, is taken with reference to the coordinates of the load point $\mathbf{X}$ i.e. it does not involve the boundary variables $\dot{\mathbf{u}}$ and $\dot{\mathbf{t}}$. The final expression of the internal stress tensor rate is:

$$\begin{aligned}\dot{\sigma}_{ij}(\mathbf{X}) = &\int_\Gamma U^*_{ijk}(\mathbf{X},\mathbf{x})\dot{t}_k(\mathbf{x})d\Gamma(\mathbf{x})\\ &-\int_\Gamma T^*_{ijk}(\mathbf{X},\mathbf{x})\dot{u}_k(\mathbf{x})d\Gamma(\mathbf{x})\\ &+\int\!\!\!\!\!\!-_\Omega \Sigma^*_{ijkl}(\mathbf{X},\mathbf{x})\dot{\sigma}^d_{kl}(\mathbf{x})d\Omega(\mathbf{x})\\ &+g_{ij}(\dot{\sigma}^d_{kl})\end{aligned} \tag{33}$$

where U^*_{ijk}, T^*_{ijk}, Σ^*_{ijkl} and g_{ij} are given in Appendix A. The differentiation of the relation (31) with respect to X_l needs the evaluation of:

$$I_{il}(\mathbf{X}) = \frac{\partial}{\partial X_l}\int_\Omega \varepsilon^*_{ijk}(\mathbf{X},\mathbf{x})\dot{\sigma}^d_{jk}(\mathbf{x})d\Omega(\mathbf{x}) \tag{34}$$

and the derivatives $\varepsilon^*_{ijk,l}(\mathbf{X},\mathbf{x})$ (where l is referred to the lth coordinate of $\mathbf{X}$) exhibit a $r^{-\dim}$ singularity, where dim is the space dimension, which is not integrable over Ω. Thus the differentiation with respect to X_l in $I_{il}(\mathbf{X})$ cannot be transferred under the integral sign. This difficulty is rather serious and it was correctly solved by Bui (1978) who established the correct expression of $I_{il}(\mathbf{X})$ involving both a free term $g_{ij}(\dot{\sigma}^d_{kl})$ and a domain integral $\int\!\!\!\!\!\!-_\Omega \Sigma^*_{ijkl}(\mathbf{X},\mathbf{x})\dot{\sigma}^d_{kl}(\mathbf{x})d\Omega(\mathbf{x})$ in the Cauchy principal value sense (see also Brebbia et al. 1984, pp. 255–258; Bonnet 1995, p. 325). The free term also contains the term $\dot{\sigma}^d_{ij}$.

The calculation of stresses at any point of Ω is of fundamental importance for the stepwise solution of nonlinear material problems; for this reason the expression of the stress tensor rate is preferred to the one of the strain tensor rate.

It must be underlined that the expression (33) is the exact value of the stress tensor rate related to the displacement-traction rate distribution $\dot{\mathbf{u}}$, $\dot{\mathbf{t}}$ on Γ, and it is not an approximate evaluation, as is the case in FE or Finite Difference (FD) approaches. Of course, the stress value will be a consequence of the assumed shape functions on the boundary.

The integral representation of the displacement rate for a boundary point $\boldsymbol{\xi}$ can be obtained by a suitable limiting process ($\mathbf{X} \to \boldsymbol{\xi}$) in which the point is an internal point surrounded by part of a spherical surface of radius ε (see Brebbia et al. 1984, pp. 191–194), i.e. by the application of the concept of Cauchy principal value of an integral. The study of the arising limits gives the following boundary integral representation of the displacement rate:

$$\begin{aligned}&c_{ij}(\boldsymbol{\xi})\dot{u}_j(\boldsymbol{\xi}) + \int\!\!\!\!\!\!-_\Gamma t^*_{ij}(\boldsymbol{\xi},\mathbf{x})\dot{u}_j(\mathbf{x})d\Gamma(\mathbf{x})\\ &\quad= \int_\Gamma u^*_{ij}(\boldsymbol{\xi},\mathbf{x})\dot{t}_j(\mathbf{x})d\Gamma(\mathbf{x})\\ &\qquad+\int_\Omega \varepsilon^*_{ijk}(\boldsymbol{\xi},\mathbf{x})\dot{\sigma}^d_{jk}(\mathbf{x})d\Omega(\mathbf{x})\end{aligned} \tag{35}$$

where the integral on the left hand side is to be interpreted in the sense of Cauchy principal value and the coefficient $c_{ij}(\boldsymbol{\xi})$ is related to the limit value (as $\varepsilon \to 0$) of the integral of the fundamental solution t^*_{ij} on the semi-circle line surrounding $\boldsymbol{\xi}$ (see for instance Aliabadi 2002, pp. 36–37), being equal to 0.5 if the tangent line at $\boldsymbol{\xi}$ is continuous. Equation 35 furnishes an integral equation involving boundary variables only, i.e. displacement and traction vector rates.

Relation (33) was deduced for points located within the body, therefore it cannot be used to determine the boundary stress rates. The limit of such an integral representation when the load point $\mathbf{X}$ goes to the boundary can be taken in a similar manner to the boundary displacement equation. However, the resulting integral:

$$\int\!\!\!\!\!\!-_\Gamma T^*_{ijk}(\boldsymbol{\xi},\mathbf{x})\dot{u}_k(\mathbf{x})d\Gamma(\mathbf{x}) \tag{36}$$

would contain a hypersingularity, hence a more sophisticated integration technique would be required and therefore an increase in the CPU time would arise.

Besides, all the strategies proposed in literature in regularising the hypersingular term, i.e. partial regularisation presented by Sládek and Sládek (1983), complete or indirect regularisation by Krishnasamy et al. (1992) and exact integration by Salvadori (2002) and by Zhang and Zhang (2004), require the displacement field and the unit normal to possess $C_{1,\alpha}$ and $C_{0,\alpha}$ smoothness, respectively, at the collocation point $\boldsymbol{\xi}$.

On the other hand, the stress tensor rates at any boundary point $\boldsymbol{\xi}$ can be expressed in terms of boundary tractions and displacements and by strain component along the tangent direction to the boundary. Details of the procedure and final relations in 2-D are given in Appendix B.

The displacement rate boundary integral equation (35), the expression both of the internal stress tensor rate (33) and of the boundary stress tensor rate (85) are to be used in the incremental iterative solution algorithm. It is therefore necessary to set both a boundary discretisation and a domain discretisation in the region where the damage process occurs in order to evaluate the integrals involved.

It must be pointed out that (either totally or partially) discontinuous quadratic cells have also been tried for the region close to the boundary in order to avoid both a hypersingular term and the approximated boundary stress tensor rate (85). With reference to the numerical examples shown in the last section, the difference between the results obtained with the discontinuous cells and the approximated formulation (85) was negligible and the convergence was not improved.

4. The boundary/domain element incremental problem

The resolution of the rate problem requires two different discretisation techniques. The first one is related to the integration along the loading path of the rate constitutive equations, and this is achieved by the Euler backward difference scheme, the second discretisation is the space discretisation required by the BDEM. In the nonlocal approach another discretisation would be necessary in order to evaluate the nonlocal value of the variable. Nevertheless, it is more convenient from the computational point of view to use the same domain discretisation provided that such a discretisation is sufficiently fine in comparison with the adopted characteristic length.

4.1. Discretisation and singular integrals treatment

The boundary Γ is divided into N_Γ continuous three noded (quadratic) elements and the displacement and traction rates as well as the geometry can be approximated in each boundary element Γ_l by products between the shape function, $M^n_\Gamma(\eta)$, and the nodal values where η represents the local coordinate taking value $0, -1, 1$ in each element node. The domain discretisation needs to be performed only for that region $\Omega_d \subseteq \Omega$ susceptible to damage, such as areas of higher strain energy density, whereas for other numerical techniques the whole domain must be discretised. This is especially attractive in damage mechanics for brittle materials since the area expected to damage tends to the macro-crack shape. The domain Ω_d is divided into N_Ω quadratic triangular or quadrilateral cells (with shape functions $M^n_\Omega(\eta, \zeta)$) and the stress rate tensor in the local cell Ω_d can be expressed as:

$$\dot{\sigma}^d_{ij}(\mathbf{x}(\eta,\zeta)) = \sum_{n=1}^{p} M^n_\Omega(\eta,\zeta)\dot{\sigma}^{d,n}_{ij} \tag{37}$$

where $\mathbf{x} \in \Omega_d$, p is the number of nodes in the cell (6 for the triangular cell, 9 for the quadrilateral one) and $\dot{\sigma}^{d,n}_{ij}$ is the damaged stress tensor rate in the cell node n. η, ζ represent the local coordinate system in the cell. The same shape functions M^n_Ω can be used to represent the geometry of the damaged area too.

By performing both the boundary and the domain discretisation described above, the discretised displacement rate boundary integral equation at the node $\bar{\boldsymbol{\xi}}$ can be written as:

$$\begin{aligned} c_{ij}(\bar{\boldsymbol{\xi}})\dot{u}_j(\bar{\boldsymbol{\xi}}) + \sum_{l=1}^{N_\Gamma}\sum_{n=1}^{3}\dot{u}^n_j \int_{-1}^{+1} t^*_{ij}(\bar{\boldsymbol{\xi}}, \mathbf{x}(\eta)) \\ \times M^n_\Gamma(\eta) J^l(\eta) d\eta \\ = \sum_{l=1}^{N_\Gamma}\sum_{n=1}^{3}\dot{t}^n_j \int_{-1}^{+1} u^*_{ij}(\bar{\boldsymbol{\xi}}, \mathbf{x}(\eta)) M^n_\Gamma(\eta) J^l(\eta) d\eta \\ + \sum_{l=1}^{N_\Omega}\sum_{n=1}^{p}\dot{\sigma}^{d,n}_{jk} \int_{-1}^{+1}\int_{-1}^{+1} \varepsilon^*_{ijk}(\bar{\boldsymbol{\xi}}, \mathbf{x}(\eta,\zeta)) M^n_\Omega(\eta,\zeta) \\ \times J^l(\eta,\zeta) d\eta d\zeta \end{aligned} \tag{38}$$

where $\dot{\mathbf{u}}^n, \dot{\mathbf{t}}^n$ represent the values of displacement and traction rates respectively in each of the three nodes of the generic boundary element with Jacobian $J^l(\eta)$, and

$J^l(\eta,\zeta)$ is the Jacobian of the generic domain cell. The expression of the stress tensor rate at the internal cell node $\overline{\mathbf{X}}$ in its discretised form can be written as:

$$\dot{\sigma}_{ij}(\overline{\mathbf{X}}) = \sum_{l=1}^{N_\Gamma}\sum_{n=1}^{3}\dot{t}_k^n \int_{-1}^{+1} U^*_{ijk}(\overline{\mathbf{X}},\mathbf{x}(\eta))M^n_\Gamma(\eta)J^l(\eta)d\eta - \sum_{l=1}^{N_\Gamma}\sum_{n=1}^{3}\dot{u}_k^n \int_{-1}^{+1} T^*_{ijk}(\overline{\mathbf{X}},\mathbf{x}(\eta))M^n_\Gamma(\eta)J^l(\eta)d\eta + \sum_{l=1}^{N_\Omega}\sum_{n=1}^{p}\dot{\sigma}_{kl}^{d,n}\ \text{p.v.}\int_{-1}^{+1}\int_{-1}^{+1}\Sigma^*_{ijkl}(\overline{\mathbf{X}},\mathbf{x}(\eta,\zeta)) \times M^n_\Omega(\eta,\zeta)J^l(\eta,\zeta)d\eta d\zeta + g_{ij}\left(\dot{\sigma}_{kl}^{d,n}\right) \quad (39)$$

where the last integral is to be taken in the Cauchy principal value (p.v.) sense.

The boundary integrals appearing in the Eqs. 38 and 39 when the source node $\overline{\boldsymbol{\xi}}$ belongs to the boundary element Γ_l are dealt with by using well established techniques. In the Eq. 38 three terms deserve special attention. The logarithmic quadrature rule is used for the singularity of order $\ln r$ contained in the term involving the fundamental displacement u^*_{ij}. The integration of the term containing the fundamental traction t^*_{ij}, containing the $1/r$ (strong) singularity along the line, can be avoided by the use of the rigid body technique (Aliabadi 2002, p. 51). The domain integral contains a weak singularity of order $1/r$ in the 2-D cell and it can be treated by performing a suitable coordinate transformation which results in an integral to be evaluated by standard Gaussian quadrature. On the other hand, concerning the Eq. 39, attention must be paid only for the domain integral which contains a strong singularity of order $1/r^2$ in the 2-D cell. It can be transformed into the sum of regular integrals by applying the same coordinate transformation of the previous weakly singular domain integral and by introducing a Taylor series expansion about the collocation point. The method was proposed by Guiggiani and Gigante (1990) in its general form. Details of the procedure are given in Appendix C.

Evaluating nearly singular integrals is another key issue in the boundary element analysis. The problem occurs in evaluating both the boundary integrals and the domain integrals involved in the Eqs. 38 and 39 when either the collocation point is too close to the integration boundary element or the stress is evaluated very near to the boundary. Conventional Gaussian quadrature rule proves to be successful when applied in estimating the stress in points which are far from the boundary and in the displacement boundary integral equation if the collocation point is far from the boundary element, but its accuracy deteriorates tremendously in evaluating nearly singular integrals. In the present work, the method used to compute such integrals is based on the iterative element subdivision. Concerning the nearly singular boundary integrals, the element is iteratively divided in sub-elements until the minimum distance between the collocation node and the subelement itself becomes greater than its length. Eight Gauss points are used in each sub-element. On the other hand, the nearly singular domain integral is evaluated by dividing the cell in either four or sixteen sub-cells in terms of the value of the minimum distance between the collocation point and the cell; sixteen Gauss points are used in each sub-cell.

The discretised displacement rate boundary integral equation (38) along with both the discretised integral representation (39) of the internal stress tensor rate and (if continuous cells are adopted) the expression (85) of the boundary stress rate tensor are to be used in the incremental iterative solution algorithm. By the classical collocation approach and by applying the Dirichlet/Neumann boundary conditions the above relations can be written in matrix form as:

$$A\dot{\mathbf{x}} = \dot{\mathbf{f}} + Q\dot{\boldsymbol{\sigma}}^d \quad (40)$$

$$\dot{\boldsymbol{\sigma}} = -A'\dot{\mathbf{x}} + \dot{\mathbf{f}}' + (Q' + E')\dot{\boldsymbol{\sigma}}^d \quad (41)$$

the bold letters meaning vectors whereas the capital letters meaning matrices. The unknowns (either displacement or traction rate on the boundary) are collected in $\dot{\mathbf{x}}$, and A, A' and Q, Q', E' are matrices involving boundary and domain integrals of the fundamental solutions respectively.

Considering the evolution problem from a discrete incremental standpoint for a finite time step $\Delta t = t_{s+1} - t_s$, these relations can be written as:

$$A\Delta\mathbf{x}_s = \mathbf{f}\Delta\lambda_s + Q\Delta\boldsymbol{\sigma}^d_s \quad (42)$$

$$\Delta\boldsymbol{\sigma}_s = -A'\Delta\mathbf{x}_s + \mathbf{f}'\Delta\lambda_s + (Q' + E')\Delta\boldsymbol{\sigma}^d_s \quad (43)$$

where the notation $\Delta(\ )_s = (\ )_{s+1} - (\ )_s$ has been used and $\Delta\lambda_s$ represents the sth load factor increment.

4.2. The arclength technique

The classical incremental procedures that are used in BEM analyses are the load and the displacement control techniques. Both strategies assume either a load increment or a displacement increment and they evaluate the solution, which is both equilibrated with the external loads and respectful of the constitutive equations, at the end of the step by an iterative scheme. As a matter of fact, these approaches are not able to cope with special peak points, for instance when the structural response has a snap-back path. The arclength methods are intended to enable solution algorithms to pass such special limit points. Because damage models can give rise to snap-back paths, in this paper the governing integral equations described above are used together with the arclength constraint. The procedure was presented by Mallardo and Alessandri (2004) in softening plasticity. It is based on a nonlinear system of equations resolution of which is performed by the Newton-Raphson method, i.e. at every time step the iterative process evaluates in sequence $\delta\Delta\lambda$, $\delta\Delta\mathbf{x}$, and $\delta\Delta\boldsymbol{\sigma}$ where $\delta\Delta(\,) = \Delta(\,)_{new} - \Delta(\,)_{old} = \Delta(\,)_n - \Delta(\,)_o$ represents the additive correction.

Equations 42, 43 can be coupled to the classical arclength constraint and re-written in the following way:

$$\begin{aligned}\mathbf{R}(\Delta\lambda, \Delta\mathbf{x}, \Delta\boldsymbol{\epsilon}) &= A\Delta\mathbf{x} - \mathbf{f}\Delta\lambda - QC^{el}\Delta\boldsymbol{\epsilon} \\ &\quad + Q\Delta\boldsymbol{\sigma} = 0 \qquad (44)\\ \mathbf{R}'(\Delta\lambda, \Delta\mathbf{x}, \Delta\boldsymbol{\epsilon}) &= A'\Delta\mathbf{x} - \mathbf{f}'\Delta\lambda - (\overline{Q}C^{el} - C^{el})\Delta\boldsymbol{\epsilon} \\ &\quad + \overline{Q}\Delta\boldsymbol{\sigma} = 0 \qquad (45)\\ a(\Delta\lambda, \Delta\mathbf{x}) &= \Delta\mathbf{x}^T\Delta\mathbf{x} + \psi^2\Delta\lambda^2\mathbf{f}^T\mathbf{f} \\ &\quad - \Delta l^2 = 0 \qquad (46)\end{aligned}$$

where the subscript s is omitted, Δl is the fixed radius of the desired intersection between the equilibrium path and the arclength constraint, ψ is a scaling parameter which regularises the inconsistency in the physical dimensions and $\overline{Q} = Q' + E' + I$. In the numerical results presented in this paper, only one arclength control point (on the boundary) is set. If $\overline{\mathbf{u}}$ and $\overline{\mathbf{q}}$ are the displacement and the traction respectively of such a point, the Eq. 46 can be written as

$$a(\Delta\lambda, \Delta\overline{\mathbf{u}}) = \Delta\overline{\mathbf{u}}^2 + \psi^2\Delta\lambda^2\overline{\mathbf{q}}^2 - \Delta l^2 = 0 \qquad (47)$$

In case the control point is internal, some mathematical manipulations are necessary.

The Newton-Raphson method can be applied via a truncated Taylor series. In matrix form:

$$\begin{pmatrix}\mathbf{R}_o\\ \mathbf{R}'_o\\ a_o\end{pmatrix} = \begin{bmatrix}\mathbf{f} & -A & Q(C^{el}-C^t)\\ \mathbf{f}' & -A' & \overline{Q}(C^{el}-C^t) - C^{el}\\ -2\Delta\lambda_o\psi^2\mathbf{f}^T\mathbf{f} & -2\Delta\mathbf{x}_o^T & 0\end{bmatrix}\begin{pmatrix}\delta\Delta\lambda\\ \delta\Delta\mathbf{x}\\ \delta\Delta\boldsymbol{\epsilon}\end{pmatrix} \qquad (48)$$

C^t is the tangent operator, i.e. $C^t = \frac{\partial\Delta\boldsymbol{\sigma}}{\partial\Delta\boldsymbol{\epsilon}}\big|_o$ and the residual terms are given by:

$$\mathbf{R_o} = A\Delta\mathbf{x}_o - \mathbf{f}\Delta\lambda_o - Q\Delta\boldsymbol{\sigma}_o^d \qquad (49)$$

$$\mathbf{R}'_\mathbf{o} = A'\Delta\mathbf{x}_o - \mathbf{f}'\Delta\lambda_o - \overline{Q}\Delta\boldsymbol{\sigma}_o^d + \Delta\boldsymbol{\sigma} \qquad (50)$$

$$a_o = \Delta\mathbf{x}_o^T\Delta\mathbf{x}_o + \psi^2\Delta\lambda_o^2\mathbf{f}^T\mathbf{f} - \Delta l^2 \qquad (51)$$

If the tangent operator is kept constantly equal to the elastic one C^{el} along the iterations, the system of equations can be easily uncoupled in three relations which can be evaluated separately to give the additive corrections at every step. On the contrary, if either a full or a modified Newton-Raphson approach is adopted, the system of nonlinear equations (48) needs to be investigated to obtain more cumbersome relations. From the first two relations of the Eq. 48 it is possible to derive the expression of both the elastic stress and the boundary unknown additive corrections:

$$\delta\Delta\mathbf{x} = A^{-1}\left[-\mathbf{R}_o + \mathbf{f}\delta\Delta\lambda + Q\overline{C}\delta\Delta\boldsymbol{\sigma}^{el}\right] \qquad (52)$$

$$\delta\Delta\boldsymbol{\sigma}^{el} = (I - \overline{Q}\,\overline{C})^{-1}(-\mathbf{R}'_o - A'\delta\Delta\mathbf{x} + \mathbf{f}'\delta\Delta\lambda) \qquad (53)$$

where:

$$\overline{C} = I - C^t C^{el^{-1}}. \qquad (54)$$

Substituting the Eq. 53 into the Eq. 52 the expression of the boundary unknowns additive correction is obtained in terms of the scalar quantity $\delta\Delta\lambda$:

$$\delta\Delta\mathbf{x} = B^{-1}\left[-\mathbf{R}_o + \mathbf{f}\delta\Delta\lambda - P(\mathbf{R}'_o - \mathbf{f}'\delta\Delta\lambda)\right] \qquad (55)$$

where:

$$T = (I - \overline{Q}\,\overline{C}) \qquad (56)$$

$$P = Q\overline{C}\,T^{-1} \qquad (57)$$

$$B = A + Q\,\overline{C}\,T^{-1}A' \qquad (58)$$

In analogy with the FE context (see Crisfield 1991, p. 273), the boundary unknown additive correction can be written as:

$$\delta\Delta\mathbf{x}=\delta\Delta\mathbf{x}^{I}+\delta\Delta\lambda\delta\Delta\mathbf{x}^{II} \tag{59}$$

where

$$\delta\Delta\mathbf{x}^{I}=-B^{-1}(\mathbf{R}_o+P\mathbf{R}'_o) \tag{60}$$

$$\delta\Delta\mathbf{x}^{II}=B^{-1}(\mathbf{f}+P\mathbf{f}') \tag{61}$$

The term $\delta\Delta\mathbf{x}^{II}$ would not change along the iterations in which the global tangent matrix B is kept constant. In case a linearised form of the arclength constraint is used, the following expression of the load-parameter additive correction is obtained:

$$\delta\Delta\lambda=-\frac{1}{2}\frac{a_o+2\Delta\mathbf{x}_o^T\delta\Delta\mathbf{x}^{I}}{\psi^2\Delta\lambda_o^2\mathbf{f}^T\mathbf{f}+\Delta\mathbf{x}_o^T\delta\Delta\mathbf{x}^{II}} \tag{62}$$

On the other hand, if the quadratic form is retained, a quadratic equation in $\delta\Delta\lambda$ perfectly coincident with the one given by Crisfield (1991, pp. 273–274), is obtained. Both approaches have been attempted by the author, but no meaningful difference is encountered in the numerical examples presented in this paper. After the evaluation of the both load-parameter and boundary unknowns additive correction, the additive correction of the elastic stress increment can be evaluated by:

$$\delta\Delta\boldsymbol{\sigma}^{el}=T^{-1}(-\mathbf{R}'_o-A'\delta\Delta\mathbf{x}+\mathbf{f}'\delta\Delta\lambda) \tag{63}$$

For the iterations occurring when the damage parameter has reached values close to one for some points, it could be more convenient to start the first iteration with a reduced tangent operator rather than with the elastic one, i.e. rather with the following elastic try:

$$\delta\Delta\boldsymbol{\sigma}^{el}_{first}=-A'\Delta\mathbf{x}+\mathbf{f}'\Delta\lambda \quad \text{where} \quad \Delta\mathbf{x}=A^{-1}\mathbf{f}\Delta\lambda \tag{64}$$

The tangent operator C^t can be obtained by the stress–strain relation (1). In the linear case:

$$\Delta\boldsymbol{\sigma}=(1-d-\Delta d)C^{el}\Delta\boldsymbol{\epsilon}-\Delta dC^{el}\boldsymbol{\epsilon} \tag{65}$$

Therefore:

$$\frac{\partial\Delta\boldsymbol{\sigma}}{\partial\Delta\boldsymbol{\epsilon}}=(1-d-\Delta d)C^{el}-\frac{\partial\Delta d}{\partial\Delta\boldsymbol{\epsilon}}C^{el}(\boldsymbol{\epsilon}+\Delta\boldsymbol{\epsilon}) \tag{66}$$

In order to impose the nonlocal damage law at the end of the step, the constitutive relations are integrated by the Euler backward scheme, namely:

$$\Delta d=\frac{\overline{Y}_{s+1}-g_s}{h} \quad \text{if the damage is linear and } \psi^{nl} \text{ is given by Eq. 8} \tag{67}$$

$$\Delta d=1-d-\frac{c}{\exp\left[\left(\frac{\overline{Y}_{s+1}}{k}\right)^{\frac{1}{n}}\right]} \quad \text{if the damage is linear and } \psi^{nl} \text{ is given by Eq. 9} \tag{68}$$

It must be pointed out that the obtained expressions of the damage increment are formally equivalent to the classical local damage loading problem. This is true only in the hypothesis of linearity of the model which makes Y not dependent on damage. If a quadratic damage law were adopted, then the damage increment would be the solution of a Fredholm integral equation to be solved by more complex strategies.

The nonlocal value $\overline{Y}$ of Y in the generic domain point $\mathbf{X}$ can be evaluated at every iteration step by the Gauss integration rule:

$$\overline{Y}(\mathbf{X})=\frac{1}{\overline{W}(\mathbf{X})}\sum_{l=1}^{N_\Omega}\sum_{ig_1=1}^{n_{g1}}\sum_{ig_2=1}^{n_{g2}}w_{ig_1}w_{ig2}J_l \times\exp\left[-\frac{\|\mathbf{X}-\mathbf{y}_g\|}{2l^2}\right]\sum_{n=1}^{p}M^n_\Omega(\eta_{ig_1},\zeta_{ig_2})Y_n \tag{69}$$

where $\overline{W}(\mathbf{X})$ is equal to the relation obtained from the Eq. 69 by posing $Y_n=1$ for every n. In the classical physically nonlinear BDEM approach, the domain discretisation is limited to the part of the domain where the nonlinear phenomenon occurs, i.e. $\Omega_d\subseteq\Omega$.

5. Numerical examples

Some numerical examples are presented in order to show the efficiency of the procedure. The first example refers to the rectangular plate in Fig. 2 where a plane stress behaviour is adopted and the measures are given in millimeters. The second numerical application concerns the direct traction depicted in Fig. 12: a constant displacement is applied at the top side of the plate in plane stress condition.

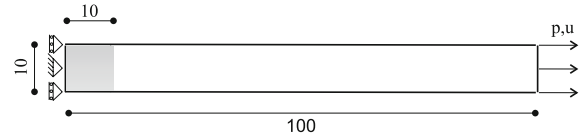

Fig. 2 Example 1. Geometry and load condition

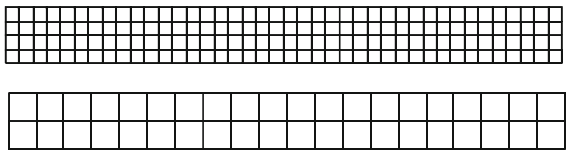

Fig. 3 Example 1. Domain discretisation

5.1. Example 1

The present example is a useful benchmark, often adopted in the FE context, which is able to show clearly the onset of the localisation and the effect of the nonlocal regularisation approach.

The Young's modulus and the Poisson's coefficient are respectively $E = 36,000$ MPa and $\nu = 0$. The null value of the Poisson's coefficient is able to keep the mechanical behaviour as one-dimensional even in the nonlinear branch.

The mechanical parameters assigned are $h = 0.02$ MPa, $Y_0 = 0.01$ MPa and $k = 1.5E-4$ MPa, $c = 2.7$, $n = 2$. In order to trigger the damage localisation, the part of the plate in grey presents either Y_0 or k reduced of 5%.

Two different discretisations are adopted: 20×2 and 40×4 quadratic quadrilateral elements (Fig. 3).

The boundary discretisation is carried out in order to have the coincidence between the boundary elements and the side of the domain cells coincident with the contour. It must be pointed out that in this example the damage may be diffused over the entire bar and, therefore, one of the main advantages of the BDEM, i.e. the possibility of discretising only the part of domain affected by the damage, is not evident. In different situations, in which the geometry and the load conditions reproduce some stress concentrations, the damage will be localised in a more narrow area, and the domain cells will be introduced only in a small zone.

The characteristic length is assumed to be $l_c = 20$ mm.

Figure 4 presents the structural response in terms of p, u with reference to the local model in which ψ^{nl} is given by the Eq. 5. The procedure becomes unstable once the damage activates in the grey area, i.e. the model is not able to spread the damage over the bar. The lost of convergence occurs for both the meshes. Figures 5 and 6 show respectively the structural response and the damage distribution if the model described by Eq. 5 is regularised by the presented nonlocal approach. The

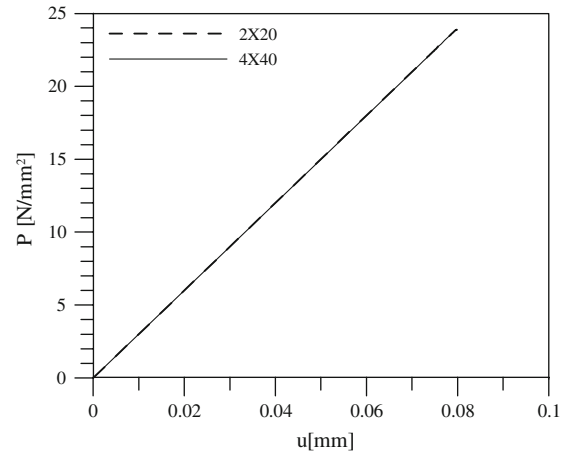

Fig. 4 Example 1. Global p, u response. Local model. $X = X_1$

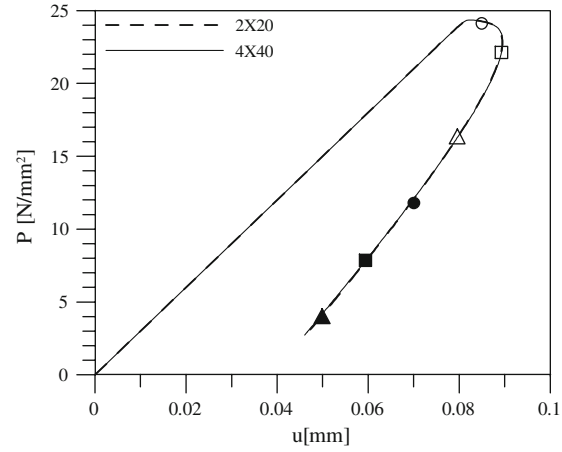

Fig. 5 Example 1. Global p, u response. Nonlocal model. $X{=}X_1$

damage distribution depicted in Fig. 6 refers to the points of the equilibrium path represented by the same symbol in the structural response of Fig. 5. The response is independent of the mesh, the damage propagates correctly outside the weaker area but the behaviour turns out to be fragile. A snap-back occurs and it is well captured by the proposed arclength technique.

In the FE context, for linear elements, some Authors (see for instance Jirásek 1999) have addressed the appearance of stress oscillation patterns. Such a phenomenon is not encountered in the present formulation as Fig. 7 shows; the various stress levels are related to the position in Fig. 5 marked by the same symbol.

In the F.E. context the lack of oscillation is mainly deputed to the quadratic form of the shape functions

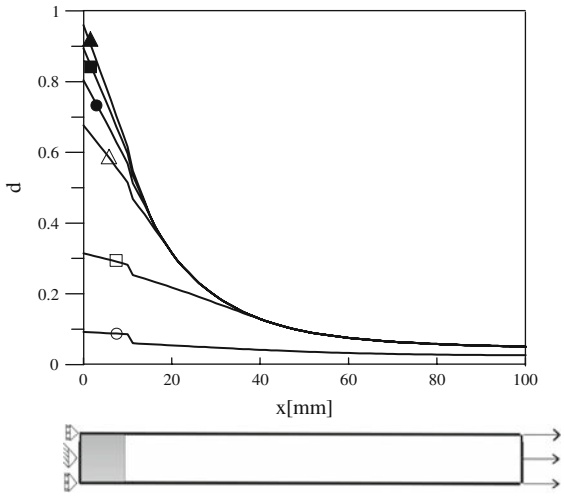

Fig. 6 Example 1. Damage distribution. Nonlocal model. $X=X_1$

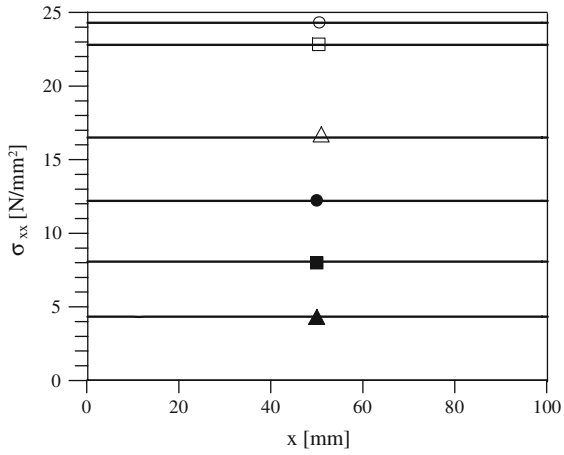

Fig. 7 Example 1. Profile of the stress. Nonlocal model. $X=X_1$

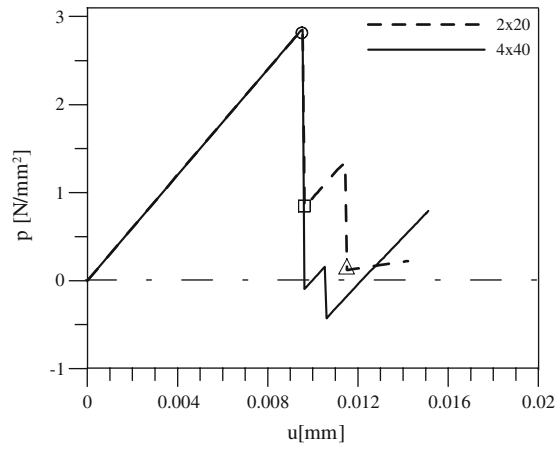

Fig. 8 Example 1. Global p, u response. Local model. $X = X_2$

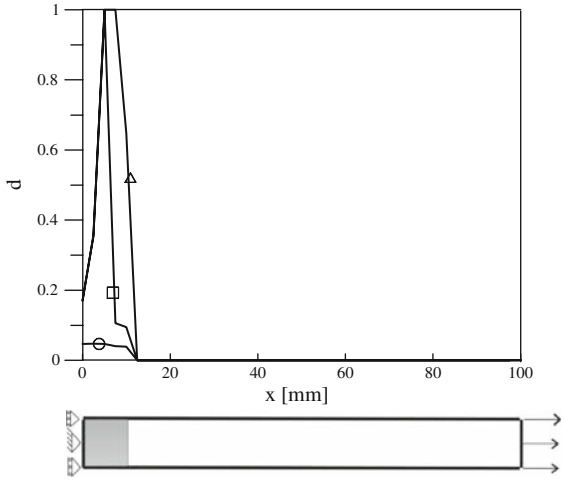

Fig. 9 Example 1. Damage distribution. Local model. $X = X_2$

adopted. In the B.E. context, the integral representation of the stress, Eq. 33, has a positive influence on the lack of oscillation.

Figures 8 and 9 show respectively the global response and the damage distribution for the model given by the Eq. 6 in the local version. Again, Fig. 9 illustrates the damage distribution at each of the equilibrium points indicated in Fig. 8 by the corresponding symbol.

The structural response presents a softening branch with jumps which demonstrates the localisation of the damage in some nodes of the weaker area. The damage distribution confirms such a behaviour: every step in the global response corresponds to a new node in which the damage parameter reaches the unity. The regularising effect of the nonlocal approach is shown in the Figs. 10 and 11 (the meaning of the symbols is the same of the previous graphics) where the response turns out to be mesh-independent and the damage spreads correctly over the bar. Two iterations and a few tenths of second (for instance 0.3 s for the finer mesh) for every arclength step are necessary to obtain the convergence with a tolerance of the order 10^{-6}. Such a tolerance refers both to the convergence in the resolution of the nonlinear system of equations inside the arclength step and to the convergence in obtaining the increment of the damage parameter. CPU time increases enormously (about 100 times slower) if the tangent approach is adopted. The increase in CPU time is mainly related to the update of

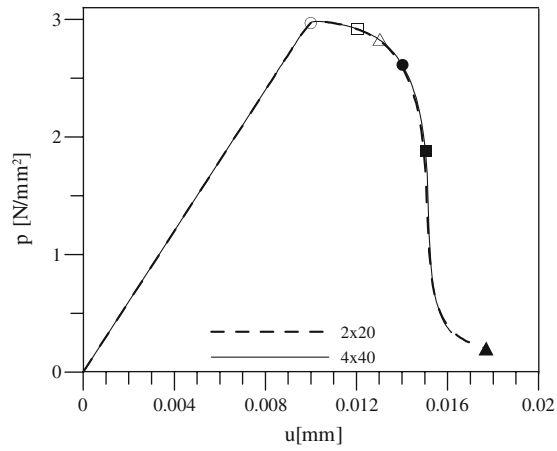

Fig. 10 Example 1. Global p, u response. Nonlocal model. $X = X_2$

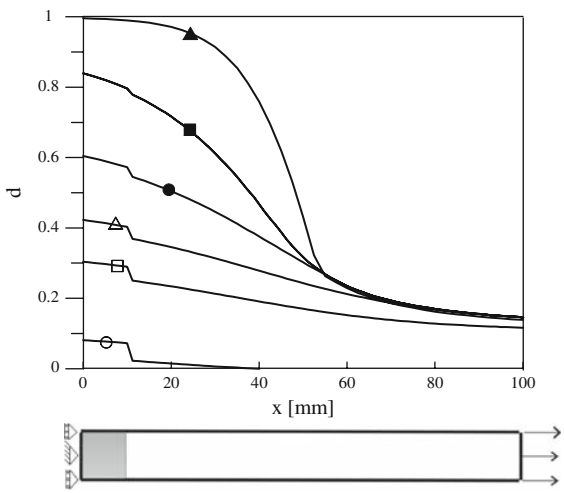

Fig. 11 Example 1. Damage distribution. Nonlocal model. $X{=}X_2$

C^t in the Eq. 48. This change, even though it does not involve the entire matrix, is very time-consuming. In the presented numerical results the matrix is updated at the first iteration of every arclength step and then it is kept constant.

5.2. Example 2

This example reproduces numerically a direct traction test of a four notched plate. Figure 12 shows the geometry and the loading condition of the sample. A constant displacement is applied at the top side of the plate; consequently the unknown pressure with R as its resultant,

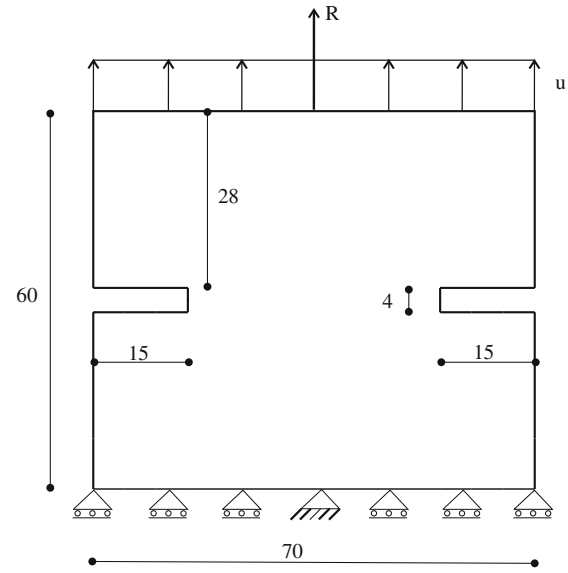

Fig. 12 Example 2. Geometry and load condition

is not distributed constantly. The numerical analysis is carried out under the hypothesis of plane stress condition and $X = X_2$. The following material parameters, corresponding to a tensile strength $\sigma_t = 3.00\,\text{MPa}$, are adopted: $E{=}36,000\,\text{MPa}$, $\nu{=}0.15$, $k{=}5.8E-14\,\text{MPa}$, $c = 405$, $n = 12$. The analysis has been performed for two different meshes shown in Fig. 13. It must be underlined that if the tangent operator C^t is kept constantly equal to the elastic one C^{el} along the iterations, i.e. $\overline{C} = 0$ in Eqs. 52, 53 and 58, the domain discretisation does not affect the matrices to be inverted.

The figures corresponding to the numerical results of the nonlocal analysis are obtained by employing the Gauss function given by Eq. 20 with the following internal length $l_c = 1.6\,\text{mm}$.

The numerical results are presented in terms of the structural response, i.e. resultant reaction R at the side where the displacement u is imposed versus u, and in terms of the damage distribution at different load levels. Such results show that the damage starts at the notches, it propagates towards the central zone of the plate and finally it extends up to the formation of a horizontal damage band. As expected, the local model is not able to capture the correct physical behaviour. Figure 14 presents the damage contour map related to the local solution obtained with both meshes at quasi-zero resistance ($R \approx 10\,\text{N/mm}^2$, $u \approx 0.007\,\text{mm}$). The damage does not spread over the central line but

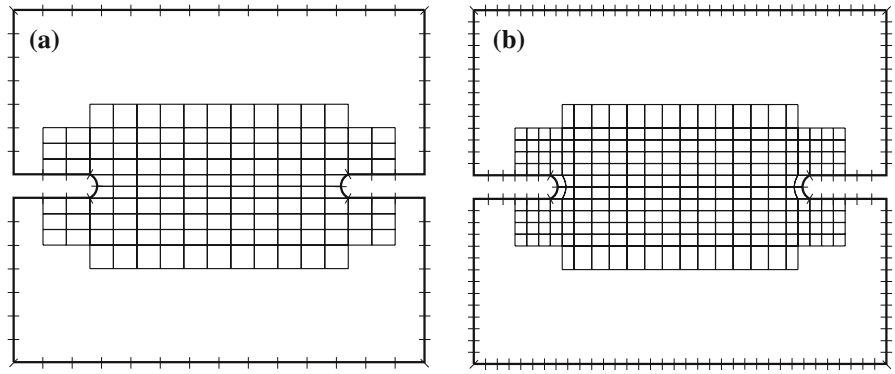

Fig. 13 Example 2. Meshes adopted in the boundary/domain elements simulations. Mesh (**a**): 72 boundary elements and 134 internal cells. Mesh (**b**): 154 boundary elements and 236 internal cells

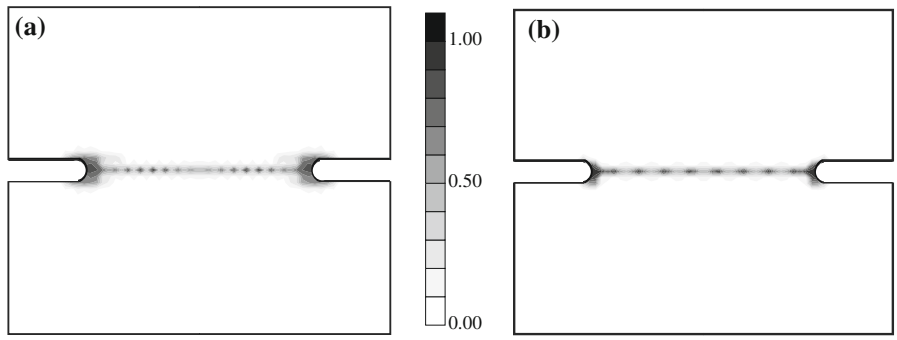

Fig. 14 Example 2. Damage contour maps related to the local solution for coarse mesh (**a**) and fine mesh (**b**)

it remains confined to a thin line the size of which changes with the adopted mesh. The peak value determined numerically turns out to be lower than the value obtained by the nonlocal analysis. In fact, the central line of the plate, where, as is evident from Fig. 14, d turns out to be close to 1, arises soon after the first occurring damage at the notches; as a consequence, the structural response moves along the softening path almost contemporarily to the appearance of the nonlinear phase, thus the peak value remains low. The integral type regularisation is evident in Fig. 15 where the structural response for the two meshes is depicted. Both meshes give the same results even though the coarser mesh is not able to capture the phenomenon when the damage parameter approaches the unit value: the number of iterations increases enormously up to the lack of satisfaction of the fixed tolerances; the result does not change significantly by using the full Newton-Raphson approach to solve Eq. 48; such a drawback is probably related to the fact that the mesh is too coarse to capture the propagation of the nonlinear phase when the damage approaches the complete detachment.

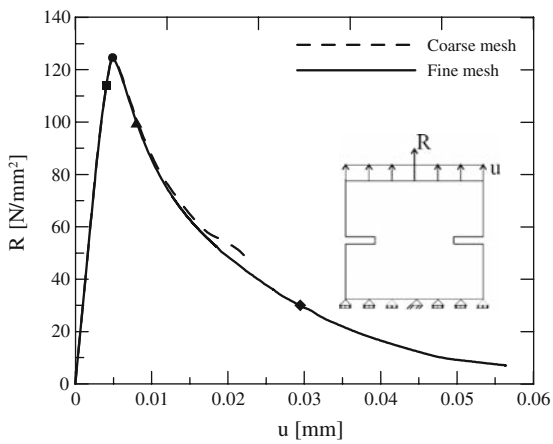

Fig. 15 Example 2. Structural response of the slab—R versus u. Nonlocal approach

Figure 16 shows the regularised damage contours at four different load levels. Such load levels are reported in Fig. 15 with the same symbols as in the structural response. The contour plots (a, b) describe the damaged zones close to the peak point and at the peak point, whereas the remaining ones refer to the softening branch. As expected, the number of iteration for every arclength step depends on the type of Newton-Raphson adopted. A comparison is shown in Fig. 17

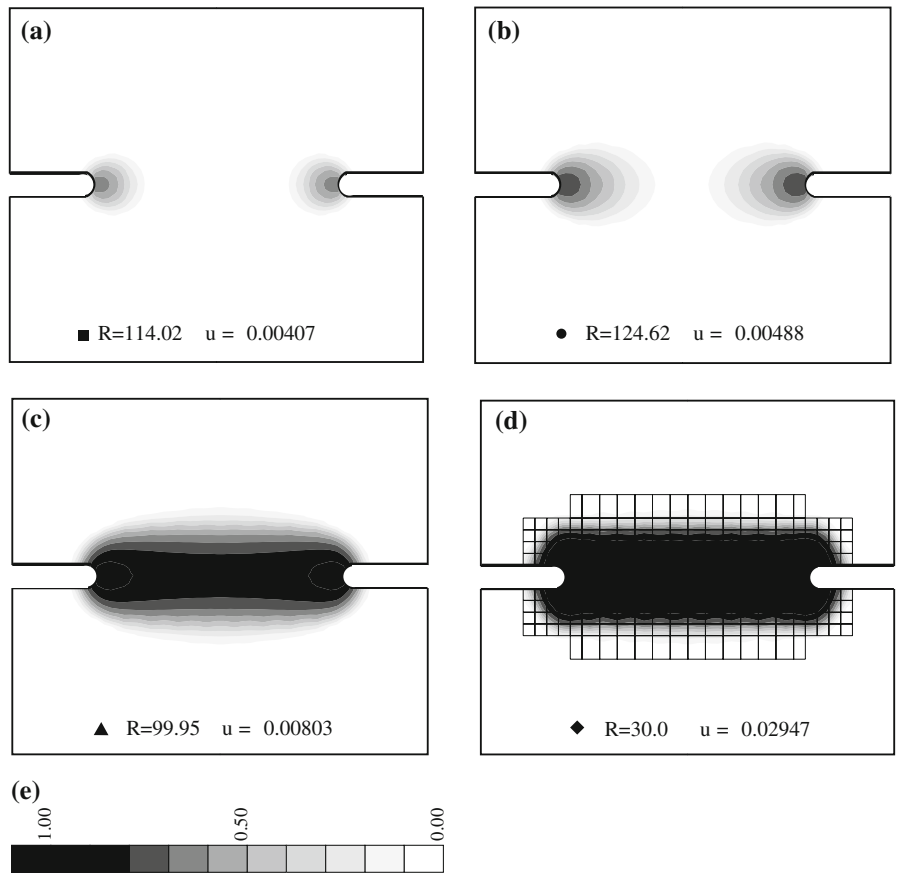

Fig. 16 Example 2. Damage contour maps corresponding to the solution obtained with the fine mesh

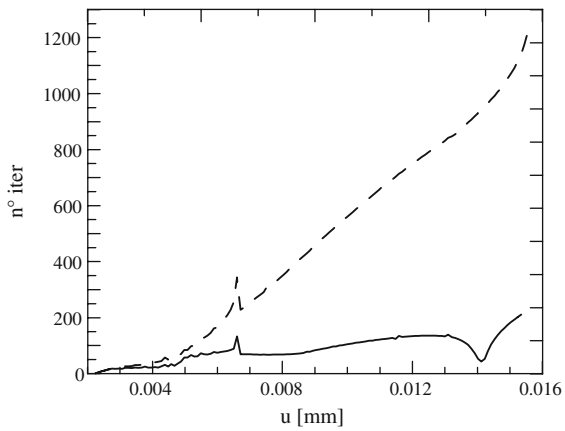

Fig. 17 Example 2. Number of iterations versus displacement u. Continuous line: C^t updated. Dashed line: C^t kept equal to the elastic value

where the number of iterations to obtain the convergence versus the value u is depicted. The x-axis starts at $u = 0.002$, i.e. where the nonlinear phase begins; of course, before that value one iteration is enough to converge to the solution. From the figure, it is clear how updating the matrix $\overline{C}$ at the beginning of every arclength step improves the rate of convergence. On the other hand, the total CPU time increases by two orders.

6. Conclusions

An integral approach for some nonlocal damage models has been presented. The formulation is physically nonlinear and thus requires the domain discretisation of the part of the volume in which the damage is expected to occur. Two simple damage models have been tested, the former more fragile than the latter. Numerical results both in 1-D and in 2-D have been obtained and discussed. The numerical results refer both to the local approach and to the nonlocal approach. The local approach has showed its inability to correctly describe

softening behaviours. A nonlocal integral type operator has been introduced in order to regularise the models. Such an integral operator has been tested both in the symmetric and in the nonsymmetric form and it has produced coincident results. In order to take into account possible snap-back branches in the structural response a coupling technique between BDEM and arclength constraints has been applied. The tangent operator involved in the Newton-Raphson procedure applied at the governing nonlinear system of equations has been either updated at the beginning of every arclength step or kept constantly equal to the elastic one.

The discretisation of the boundary and of the part of the domain affected by the damage has been performed respectively by quadratic lines and by quadratic cells. Such a choice gives a more precise representation of the damage distribution with respect to linear elements and it better describes the high damage gradient which usually occurs in such models. The BDEM approach turns out to be efficient and it only requires the discretisation of the part of the domain where the damage occurs.

Appendix A

The expression of the fundamental solutions involved in Sect. 3 for 2-D plane strain problems is given by:

$$u^*_{ij}(\mathbf{X},\mathbf{x}) = -\frac{1}{8\pi(1-\nu)\mu}\left[(3-4\nu)\delta_{ij}\ln r - r_{,i}r_{,j}\right] \tag{70}$$

$$t^*_{ij}(\mathbf{X},\mathbf{x}) = -\frac{1}{4\pi(1-\nu)r}\left\{\left[(1-2\nu)\delta_{ij}+2r_{,i}r_{,j}\right]r_{,n} - (1-2\nu)(r_{,i}n_j - r_{,j}n_i)\right\} \tag{71}$$

$$\varepsilon^*_{ijk}(\mathbf{X},\mathbf{x}) = -\frac{1}{8\pi\mu(1-\nu)r}\left[(1-2\nu)(r_{,j}\delta_{ki}+r_{,i}\delta_{jk}) - r_{,k}\delta_{ij}+2r_{,i}r_{,j}r_{,k}\right] \tag{72}$$

$$U^*_{ijk}(\mathbf{X},\mathbf{x}) = \frac{1}{4\pi(1-\nu)r}\left[(1-2\nu)(r_{,j}\delta_{ik}+r_{,i}\delta_{jk} - r_{,k}\delta_{ij})+2r_{,i}r_{,j}r_{,k}\right] \tag{73}$$

$$T^*_{ijk}(\mathbf{X},\mathbf{x}) = \frac{\mu}{2\pi(1-\nu)r^2}\left\{2r_{,n}\left[(1-2\nu)\delta_{ij}r_{,k} + \nu(\delta_{ik}r_{,j}+\delta_{jk}r_{,i}) - 4r_{,i}r_{,j}r_{,k}\right] + 2\nu(n_i r_{,j}r_{,k} + n_j r_{,i}r_{,k}) + (1-2\nu)(2n_k r_{,i}r_{,j} + n_j\delta_{ik} + n_i\delta_{jk}) - (1-4\nu)n_k\delta_{ij}\right\} \tag{74}$$

$$\Sigma^*_{ijkl}(\mathbf{X},\mathbf{x}) = \frac{1}{4\pi(1-\nu)r^2}\left\{(1-2\nu)\left[\delta_{ik}\delta_{jl} + \delta_{jk}\delta_{il} - \delta_{ij}\delta_{kl} + 2\delta_{ij}r_{,k}r_{,l}\right] + 2\nu\left[\delta_{il}r_{,j}r_{,k} + \delta_{jk}r_{,i}r_{,l} + \delta_{ik}r_{,l}r_{,j} + \delta_{jl}r_{,i}r_{,k}\right] + 2\delta_{kl}r_{,i}r_{,j} - 8r_{,i}r_{,j}r_{,k}r_{,l}\right\} \tag{75}$$

$$g_{ij}(\boldsymbol{\sigma}^d) = -\frac{1}{8(1-\nu)}\left[2\sigma^d_{ij} + (1-4\nu)\sigma^d_{mm}\delta_{ij}\right] \quad m = 1,2 \tag{76}$$

The plane strain expressions are valid for plane stress if ν is replaced by $\overline{\nu} = \frac{\nu}{1+\nu}$. In the above relations $\mathbf{X}$ and $\mathbf{x}$ are usually referred to as source point and field point respectively and $r(\mathbf{X},\mathbf{x})$ represents their distance. The involved derivatives of r are taken with respect to the coordinates of $\mathbf{x}$.

Appendix B

The global stress components at a boundary point can be partially retrieved by expressing the traction vectors in a local coordinate system and employing the relationship between strain and displacement on the tangent directions to the boundary. The procedure was developed by Lachat (1975) in elasticity and can be here extended to the proposed damage model. The relations will be obtained in 2-D. Let us assume a general boundary part with a local Cartesian coordinate system tangent to its line (see Fig. 18). It is easy to obtain components σ_{nn} and σ_{ns} of the stress tensor in terms of the traction components and of the normal and tangential vector components by applying the transformation rule:

$$\sigma_{nn} = \sigma_{ij}n_i n_j = (\sigma_{11}n_1+\sigma_{12}n_2)n_1 + (\sigma_{21}n_1+\sigma_{22}n_2)n_2 = t_1 n_1 + t_2 n_2 \tag{77a}$$

$$\sigma_{ns} = \sigma_{ij}n_i s_j = t_1 s_1 + t_2 s_2 \tag{77b}$$

where $s_1 = -n_2$ and $s_2 = n_1$. The remaining component σ_{ss} of the stress tensor can be obtained in terms of

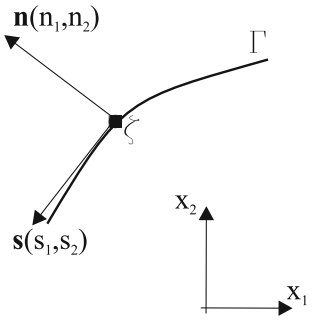

Fig. 18 Boundary point $\boldsymbol{\zeta}$. Local and global coordinate system

both the normal component of the stress and the tangential strain by manipulating the Hooke's law in plane strain ($\varepsilon_{zz} = 0$) and in the local coordinate system:

$$\sigma_{ss} = 2\mu\varepsilon_{ss}^{el} + 2\mu\frac{\nu}{1-2\nu}(\varepsilon_{ss}^{el} + \varepsilon_{nn}^{el}) \tag{78}$$

The relations

$$\varepsilon_{ss}^{el} = \varepsilon_{ss} - \varepsilon_{ss}^{d} \qquad \varepsilon_{nn}^{el} = \varepsilon_{nn} - \varepsilon_{nn}^{d} \tag{79}$$

can be substituted into the Eq. 78. It must be kept in mind that the normal strain component is given by:

$$\varepsilon_{nn} = \frac{1}{2\mu}\left[\sigma_{nn}^{el} - \nu(\sigma_{nn}^{el} + \sigma_{ss}^{el})\right] \tag{80}$$

and the elastic stress tensor can be expressed in terms of both the actual stress tensor and the damaged strain tensor by:

$$\sigma_{nn}^{el} = \sigma_{nn} + \sigma_{nn}^{d} \qquad \sigma_{ss}^{el} = \sigma_{ss} + \sigma_{ss}^{d} \tag{81}$$

and by:

$$\sigma_{nn}^{d} = 2\mu\left[\varepsilon_{nn}^{d} + \tfrac{\nu}{1-2\nu}(\varepsilon_{ss}^{d} + \varepsilon_{nn}^{d})\right] \tag{82a}$$

$$\sigma_{ss}^{d} = 2\mu\left[\varepsilon_{ss}^{d} + \tfrac{\nu}{1-2\nu}(\varepsilon_{ss}^{d} + \varepsilon_{nn}^{d})\right] \tag{82b}$$

The final expression can be arranged in the form:

$$f(\varepsilon_{ss}, \varepsilon_{ss}^{d}, \varepsilon_{nn}^{d}, \sigma_{nn}, \sigma_{ss}) = 0 \tag{83}$$

and solved in terms of σ_{ss} to obtain the requested relation:

$$\sigma_{ss} = \frac{1}{1-\nu}(2\mu\varepsilon_{ss} + \nu\sigma_{nn}) - \frac{2\mu}{1-\nu}\varepsilon_{ss}^{d} \tag{84}$$

It is possible to transform the stress tensor formed by the terms (77a–77b) and (84) from the local coordinate to the global coordinate system. The final expression of the stress tensor at any boundary point $\boldsymbol{\zeta}$ is:

$$\begin{aligned}
\begin{pmatrix}\sigma_{11}(\boldsymbol{\zeta})\\ \sigma_{22}(\boldsymbol{\zeta})\\ \sigma_{12}(\boldsymbol{\zeta})\end{pmatrix} &= \frac{2\mu}{1-\nu}\,\varepsilon_{ss}\begin{bmatrix} n_2^2\\ n_1^2\\ -n_1n_2\end{bmatrix}\\
&+\begin{bmatrix} n_1^3+n_1n_2^2+\frac{1}{1-\nu}n_1n_2^2 & -n_1^2n_2+\frac{\nu}{1-\nu}n_2^3\\ -n_1n_2^2+n_1^3\frac{\nu}{1-\nu} & n_2^3+n_1^2n_2+\frac{1}{1-\nu}n_1^2n_2\\ n_2^3-\frac{\nu}{1-\nu}n_1^2n_2 & n_1^3-\frac{\nu}{1-\nu}n_1n_2^2\end{bmatrix}\\
&\times\begin{pmatrix}t_1(\boldsymbol{\zeta})\\ t_2(\boldsymbol{\zeta})\end{pmatrix}\\
&+\begin{bmatrix} n_2^2(-n_2^2+\frac{\nu}{1-\nu}n_1^2) & n_2^2(-n_1^2+\frac{\nu}{1-\nu}n_2^2) & n_1n_2^3\frac{2}{1-\nu}\\ n_1^2(-n_2^2+\frac{\nu}{1-\nu}n_1^2) & n_1^2(-n_1^2+\frac{\nu}{1-\nu}n_2^2) & n_1^3n_2\frac{2}{1-\nu}\\ n_1n_2(n_2^2-\frac{\nu}{1-\nu}n_1^2) & n_1n_2(n_1^2-\frac{\nu}{1-\nu}n_2^2) & -n_1^2n_2^2\frac{2}{1-\nu}\end{bmatrix}\\
&\times\begin{pmatrix}\sigma_{11}^{d}(\boldsymbol{\zeta})\\ \sigma_{22}^{d}(\boldsymbol{\zeta})\\ \sigma_{12}^{d}(\boldsymbol{\zeta})\end{pmatrix}
\end{aligned} \tag{85}$$

where ε_{ss} can be evaluated by differentiating the shape functions:

$$\varepsilon_{ss} = \frac{2}{Jacob}\left[-\sum_{n=1}^{3}\frac{\partial M_{\Gamma}^{n}(\eta)}{\partial\eta}\,u_1^n\,n_2 + \sum_{n=1}^{3}\frac{\partial M_{\Gamma}^{n}(\eta)}{\partial\eta}\,u_2^n\,n_1\right] \tag{86}$$

The derivatives of the shape functions at the boundary nodes between two elements have been evaluated both as belonging to one element only and by averaging the values obtained from the two elements. For the examples presented in the paper no difference in the results has been detected.

The expression (85), slightly different from the one developed in plasticity, is valid for plane stress too provided that ν is replaced by $\overline{\nu} = \frac{\nu}{1+\nu}$. Concerning to this, it is possible to demonstrate that Eq. 78 is valid for plane stress too.

Appendix C

First of all a polar coordinate transformation is introduced in the cell:

$$\eta = \eta_0 + \rho\cos\vartheta \qquad \zeta = \zeta_0 + \rho\sin\vartheta \tag{87}$$

where η_0, ζ_0 represent the local coordinates of the source node $\overline{\boldsymbol{\xi}}$. Therefore the limits of $\rho\,(0, \overline{\rho}(\vartheta))$ and of $\vartheta\,(\vartheta_i, \vartheta_f)$ depend on the position of the source node in the integration cell and it is easy to show that the Jacobian of the transformation is given by ρ. It is possible to transform the integration limits into $-1, +1$ both for

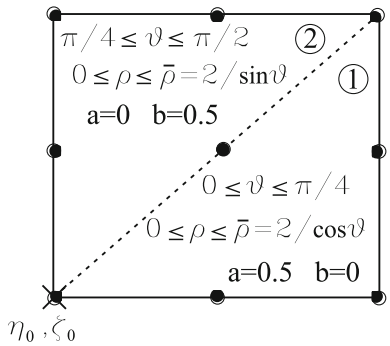

Fig. 19 Polar coordinates ρ, ϑ centered at the singular point $\overline{\boldsymbol{\xi}}$

ϑ and for ρ. The limits $(\vartheta_i, \vartheta_f)$ are transformed into $(-1, +1)$ by the Jacobian:

$$J_\vartheta = \frac{\vartheta_f - \vartheta_i}{2} \tag{88}$$

whereas the integration along ρ is transformed by the following Jacobian:

$$J_\rho = \frac{1}{2\left[a(\overline{\boldsymbol{\xi}}, \mathbf{x})\cos\vartheta + b(\overline{\boldsymbol{\xi}}, \mathbf{x})\sin\vartheta\right]} \tag{89}$$

where a and b depend on the position of the source and field nodes and they can assume only one of the values $-1, -0.5, 0, 0.5, 1$. Fig. 19 shows the case of the singular node $\overline{\boldsymbol{\xi}}$ coincident with the left bottom node of a quadrilateral cell; similar relations can be obtained in the remaining possibilities and in the case of a triangular cell.

Keeping in count the above transformation, the weekly singular domain integral in the Eq. 38 can be written as:

$$\begin{aligned}
&\int_{-1}^{+1}\int_{-1}^{+1} \varepsilon^*_{ijk}(\overline{\boldsymbol{\xi}}, \mathbf{x}(\eta,\zeta)) M^n_\Omega(\eta,\zeta) J^l(\eta,\zeta) d\eta d\zeta \\
&= \int_{-1}^{+1}\int_{-1}^{+1} \varepsilon^*_{ijk}(\overline{\boldsymbol{\xi}}, \mathbf{x}(\rho,\vartheta)) M^n_\Omega(\rho,\vartheta) \\
&\quad \times J^l(\rho,\vartheta) J_\vartheta J_\rho \rho d\rho d\vartheta
\end{aligned} \tag{90}$$

and it can be evaluated by the standard Gaussian quadrature rule, whereas the strongly singular integral:

$$\begin{aligned}
&\text{p.v.}\int_{-1}^{+1}\int_{-1}^{+1} \Sigma^*_{ijkl}(\overline{\mathbf{X}}, \mathbf{x}(\eta,\zeta)) M^n_\Omega(\eta,\zeta) J^l(\eta,\zeta) d\eta d\zeta \\
&= \text{p.v.}\int_{\vartheta_i}^{\vartheta_f}\int_0^{\overline{\rho}(\vartheta)} \Sigma^*_{ijkl}(\overline{\mathbf{X}}, \mathbf{x}(\rho,\vartheta)) M^n_\Omega(\rho,\vartheta) \\
&J^l(\rho,\vartheta)\rho d\rho d\vartheta \\
&= \text{p.v.}\int_{\vartheta_i}^{\vartheta_f}\int_0^{\overline{\rho}(\vartheta)} S_{ijkl}(\rho,\vartheta) d\rho d\vartheta
\end{aligned} \tag{91}$$

needs a further manipulation to be evaluated. The term $S_{ijkl}(\rho, \vartheta)$ can be expanded into a Taylor series expansion about the collocation point $\overline{\mathbf{X}}$ and for the components of the distance $r = \mathbf{x} - \overline{\mathbf{X}}$:

$$\begin{aligned}
r_i &= (x_{i,\eta}\,|_{\overline{\mathbf{X}}}\cos\vartheta + x_{i,\zeta}\,|_{\overline{\mathbf{X}}}\sin\vartheta)\rho + O(\rho^2) \\
&= T_i(\vartheta)\rho + O(\rho^2)
\end{aligned} \tag{92a}$$

$$r = \rho\sqrt{\sum_{i=1}^{2} T_i^2(\vartheta)} + O(\rho^2) = r_\rho + O(\rho^2) \tag{92b}$$

$$\begin{aligned}
r_{,i} &= \frac{T_i(\vartheta)}{\sqrt{\sum_{i=1}^2 T_i^2(\vartheta)}} + O(\rho) \\
&= T_i(\vartheta)T(\vartheta) + O(\rho) = r_{,i_0} + O(\rho)
\end{aligned} \tag{92c}$$

It must be pointed out that the fundamental solution strictly depends on the distance r and on the derivative $r_{,i}$ (see Eq. 75) rather than on $\overline{\mathbf{X}}$ and $\mathbf{x}$ separately, therefore if the following position:

$$s_{ijkl}(\vartheta) = \Sigma^*_{ijkl}(r_\rho, r_{,i_0}) M^n_\Omega(\overline{\mathbf{X}}) J^l(\overline{\mathbf{X}})\rho^2 \tag{93}$$

is set, then the following term:

$$\frac{s_{ijkl}(\vartheta)}{\rho} = \Sigma^*_{ijkl}(r_\rho, r_{,i_0}) M^n_\Omega(\overline{\mathbf{X}}) J^l(\overline{\mathbf{X}})\rho \tag{94}$$

has the same singular behaviour of $S_{ijkl}(\rho, \vartheta)$. Therefore the integral (91) can be re-written keeping in count the definition of the Cauchy principal value:

$$\begin{aligned}
&\text{p.v.}\int_{\vartheta_i}^{\vartheta_f}\int_0^{\overline{\rho}(\vartheta)} S_{ijkl}(\rho,\vartheta) d\rho d\vartheta \\
&= \lim_{\lambda\to 0}\int_{\vartheta_i}^{\vartheta_f}\int_{\alpha(\lambda,\vartheta)}^{\overline{\rho}(\vartheta)} S_{ijkl}(\rho,\vartheta) d\rho d\vartheta
\end{aligned} \tag{95}$$

where $\vartheta \in \left[\vartheta_i, \vartheta_f\right]$, $\rho \in [0, \alpha(\lambda, \vartheta)]$ individuates a neighbourhood of radius λ of the collocation point $\overline{\mathbf{X}}$. The limit term α is given by:

$$\alpha(\lambda, \vartheta) = \frac{\lambda}{r} = \lambda T(\vartheta) + O(\rho^2) \tag{96}$$

Adding and subtracting the term (95) the strongly singular integral becomes:

$$\begin{aligned}
&\lim_{\lambda\to 0} \int_{\vartheta_i}^{\vartheta_f} \int_{\alpha(\lambda,\vartheta)}^{\overline{\rho}(\vartheta)} S_{ijkl}(\rho, \vartheta) d\rho d\vartheta \\
&= \lim_{\lambda\to 0} \left[\int_{\vartheta_i}^{\vartheta_f} \int_{\alpha(\lambda,\vartheta)}^{\overline{\rho}(\vartheta)} \left(S_{ijkl}(\rho, \vartheta) - \frac{s_{ijkl}(\vartheta)}{\rho} \right) d\rho d\vartheta \right. \\
&\qquad \left. + \int_{\vartheta_i}^{\vartheta_f} \int_{\alpha(\lambda,\vartheta)}^{\overline{\rho}(\vartheta)} \frac{s_{ijkl}(\vartheta)}{\rho} d\rho d\vartheta \right]
\end{aligned} \tag{97}$$

The first integral in (97) is regular, i.e. the limit value is obtained substituting 0 to $\alpha(\lambda, \vartheta)$. The second integral can be evaluated in the ρ variable:

$$\begin{aligned}
&\lim_{\lambda\to 0} \int_{\vartheta_i}^{\vartheta_f} \int_{\lambda T(\vartheta)}^{\overline{\rho}(\vartheta)} \frac{s_{ijkl}(\vartheta)}{\rho} d\rho d\vartheta \\
&= \int_{\vartheta_i}^{\vartheta_f} s_{ijkl}(\vartheta) \left[\ln\left(\frac{\overline{\rho}(\vartheta)}{T(\vartheta)} \right) - \lim_{\lambda\to 0} \ln\lambda \right] d\vartheta \\
&= \int_{\vartheta_i}^{\vartheta_f} s_{ijkl}(\vartheta) \ln\left(\frac{\overline{\rho}(\vartheta)}{T(\vartheta)} \right) d\vartheta \\
&\quad - \lim_{\lambda\to 0} \left[\ln\lambda \int_{\vartheta_i}^{\vartheta_f} s_{ijkl}(\vartheta) d\vartheta \right]
\end{aligned} \tag{98}$$

where the second term can be proved to be zero when $\overline{\overline{\mathbf{X}}}$ is an internal point. The final expression of the strongly singular integral is:

$$\begin{aligned}
&\text{p.v.} \int_{-1}^{+1} \int_{-1}^{+1} \Sigma^*_{ijkl}(\overline{\mathbf{X}}, \mathbf{x}(\eta, \zeta)) M^n_\Omega(\eta, \zeta) J^l(\eta, \zeta) d\eta d\zeta \\
&= \int_{\vartheta_i}^{\vartheta_f} \int_{0}^{\overline{\rho}(\vartheta)} \left(S_{ijkl}(\rho, \vartheta) - \frac{s_{ijkl}(\vartheta)}{\rho} \right) d\rho d\vartheta \\
&\quad + \int_{\vartheta_i}^{\vartheta_f} s_{ijkl}(\vartheta) \ln\left(\frac{\overline{\rho}(\vartheta)}{T(\vartheta)} \right) d\vartheta
\end{aligned} \tag{99}$$

Both terms can now be evaluated by standard Gaussian quadrature rule. The number of points to be used depends on the position of the point $\overline{\overline{\mathbf{X}}}$ inside the cell, i.e. in terms of the number of subregions to be considered in the transformation (87), and it is set equal to either 14 or 12 or 10.

References

Alessandri C, Mallardo V, Tralli A (2000) Nonlocal continuum damage: a B.E.M. formulation. In: Atluri SN, Brust FW (eds) Advances in computational engineering & sciences, vol II. Tech Science Press, USA, pp 1293–1298

Aliabadi MH (2002) The boundary element method, vol 2: applications in solids and structures. Wiley, London

Bažant ZP, Jirásek M (2002) Nonlocal integral formulations of plasticity and damage: survey of progress. J Eng Mech ASCE 128:1119–1149

Benallal A, Botta AS, Venturini WS (2006) On the description of localization and failure phenomena by the boundary element method. Comput Methods Appl Mech Eng 195:5833–5856

Benvenuti E, Borino G, Tralli A (2002) A thermodynamically consistent nonlocal formulation for damaging materials. Eur J Mech A/Solids 21:535–553

Bonnet M (1995) Boundary integral equation methods for solids and fluids. Wiley, London

Borino G, Failla B, Parrinello F (2003) A symmetric nonlocal damage theory. Int J Solids Struct 40:3621–3645

Brebbia CA, Telles JCF, Wrobel LC (1984) Boundary element techniques. Springer-Verlag, NY

Bui HD (1978) Some remarks about the formulation of three-dimensional thermoelastoplastic problems by integral equations. Int J Solids Struct 14:935–939

Comi C, Perego U (2001) Numerical aspects of nonlocal damage analyses. Eur J Finite Elem 10:227–242

Crisfield MA (1991) Nonlinear finite element analysis of solids and structures, vol 1. Wiley, Chichester

Garcia R, Florez-Lopez J, Cerrolaza M (1999) A boundary element formulation for a class of non-local damage models. Int J Solids Struct 36:3617–3638

Guiggiani M, Gigante A (1990) A general algorithm for multidimensional Cauchy Principal Value integrals in the Boundary Element Method. J Appl Mech 57:906–915

Jirásek M (1998) Nonlocal models for damage and fracture: comparison of approaches. Int J Solids Struct 35:4133–4145

Jirásek M (1999) Computational aspects of nonlocal models. In: Proceedings of ECCM '99—European conference on computational mechanics, August 31–September 3, Munchen, Germany

Jirásek M, Patzak B (2002) Consistent tangent stiffness for nonlocal damage models. Comput Struct 80:1279–1293

Jirásek M, Rolshoven S (2003) Comparison of integral-type nonlocal plasticity models for strain-softening materials. Int J Eng Sci 41:1553–1602

Krajcinovic D (1996) Damage mechanics. North-Holland, Amsterdam

Krishnasamy G, Rizzo FJ, Rudolphi TJ (1992) Hypersingular boundary integral equations: their occurrence, interpretation, regularization and computation. In: Banerjee PK, Kobayashi S (eds) Developments in boundary element method, vol 7. Advanced dynamic analysis, chapter 7. Elsevier, Amsterdam

Lachat JC (1975) A further development of the boundary integral techniques for elastostatics. Ph.D. Thesis, University of Southampton

Lin FB, Yan G, Bažant ZP, Ding F (2002) Nonlocal strain-softening model of quasi-brittle materials using boundary element method. Eng Anal Bound Elem 26:417–424

Mallardo V (2004) Localisation analysis by BEM in damage mechanics. In: Leitão VMA, Aliabadi MH (eds) Advances in boundary element techniques V. EC Ltd., UK, pp 155–160

Mallardo V, Alessandri C (2004) Arc-length procedures with BEM in physically nonlinear problems. Eng Anal Bound Elem 28:547–559

Salvadori A (2002) Analytical integrations in 2D BEM elasticity. Int J Numer Methods Eng 53:1695–1719

Sfantos GK, Aliabadi MH (2007a) A boundary cohesive grain formulation for modelling intergranular microfracture in polycrystalline brittle materials. Int J Numer Methods Eng 69:1590–1626

Sfantos GK, Aliabadi MH (2007b) Multi-scale boundary element modelling of material degradation and fracture. Comput Methods Appl Mech Eng 196:1310–1329

Sládek J, Sládek V (1983) Three-dimensional curved crack in an elastic body. Int J Solids Struct 19:425–436

Sládek J, Sládek V., Bažant Z.P. (2003) Nonlocal boundary integral formulation for softening damage. Int J Numer Methods Eng 57:103–116

Zhang X, Zhang X (2004) Exact integration for stress evaluation in the boundary element analysis of two-dimensional elastostatics. Eng Anal Bound Elem 28:997–1004